Bioorganic & Medicinal Chemistry 16 (2008) 8403–8412

Contents lists available at ScienceDirect

Bioorganic & Medicinal Chemistry

journal homepage: www.elsevier.com/locate/bmc

Specific binding capacity of β-cyclodextrin with *cis* and *trans* enalapril: Physicochemical characterization and structural studies by molecular modeling

Ariana Zoppi, Mario A. Quevedo, Marcela R. Longhi *

Departamento de Farmacia, Facultad de Ciencias Químicas, Universidad Nacional de Córdoba, Ciudad Universitaria, 5000 Córdoba, Argentina

ARTICLE INFO

Article history:
Received 2 July 2008
Revised 12 August 2008
Accepted 14 August 2008
Available online 19 August 2008

Keywords:
Enalapril maleate
β-Cyclodextrin
Drug stability
NMR spectroscopy
Molecular modeling

ABSTRACT

The main objective of this work was to study an inclusion complex between enalapril (ENA), and β-cyclodextrin (β-CD). From nuclear magnetic resonance (NMR) we determined that the complex showed a 1:1 stoichiometry, with an apparent formation constant (K_C) of 439 and 290 M^{-1} for the *cis* and *trans* isomers, respectively. The molecular modeling and NMR techniques demonstrated that the aromatic moiety of ENA was inserted into the hydrophobic cavity of β-CD. When studying the chemical stability of ENA complexed to β-CD, a clear stabilizing effect was observed in both the aqueous solution and solid state.

1. Introduction

Enalapril (ENA, Fig. 1a) is the ethyl ester of the long-acting angiotensin converting enzyme inhibitor enalaprilat (ET, Fig. 1b), and is indicated for the treatment of essential and renovascular hypertension. Since the oral absorption of ENA is superior to that of ET, the former is used in oral dosage form.[1] This drug, however, suffers degradation in the solid state as a consequence of its interaction with excipients, a fact that causes an important stability problem when considering its formulation. Diketopiperazine (DKP, Fig. 1c) is its main degradation product, formed in solid state and by photodegradation in solution, while in solutions of pH 5 or above, ET is the main degradation product formed by hydrolysis.[2–8]

As stated above, the stability of ENA in the solid state is a crucial aspect in its formulation procedures, with the intramolecular nucleophilic attack by the secondary amine on the proline carboxylic group being the key step for the formation of DKP.[3] To overcome this problem, several methods have been attempted, for example, the formation of a maleate salt to reduce the attacking ability of the nitrogen atom in its amine group.[3] By means of these strategies, ENA formulation stability has been improved, but this achievement has been insufficient to assure long term stability of the formulations that are currently in use, with several reports indicating that degradation products are still a concern.[2,8,9]

Another widely used strategy to increase the stability of drugs is the formation of complexes with macromolecules, of which molecular encapsulation with cyclodextrins (CDs) constitutes an alternative for the development of new pharmaceutical dosage forms.[10–12] Considering that CDs frequently form inclusion complexes with drugs, and that the flexibility of the included molecule is considerably diminished through steric restriction and intermolecular interactions, then the preparation of inclusion complexes of ENA with CDs could restrain the possibility of an intramolecular nucleophilic attack, not only in the solid state but also in solution. Among CDs, β-cyclodextrin (β-CD, Fig. 2) is the most widely used in pharmaceutical industry, mainly due to its capability of including a wide variety of drugs, but also because of the low cost of bulk production.

Considering the above mentioned aspects, the purpose of this study was to prepare and characterize an ENA:β-CD inclusion complex, with the aim of enhancing the stability properties of the formulations currently in use. The study of the three-dimensional structure of this complex was carried out by means of experimental and theoretical techniques. Furthermore, the effects obtained regarding the stability of ENA as a consequence of its inclusion into the β-CD was studied in both the solid state and solution.

2. Results and discussion

2.1. ENA:β-CD complex structure elucidation

2.1.1. Spectroscopic studies

NMR spectroscopy is at present the most useful tool for the study of CD complexes, which provides qualitative and quantita-

* Corresponding author. Tel.: +54 351 433 4163; fax: +54 351 433 4127.
E-mail address: mrlcor@fcq.unc.edu.ar (M.R. Longhi).

0968-0896/$ - see front matter © 2008 Elsevier Ltd. All rights reserved.
doi:10.1016/j.bmc.2008.08.032

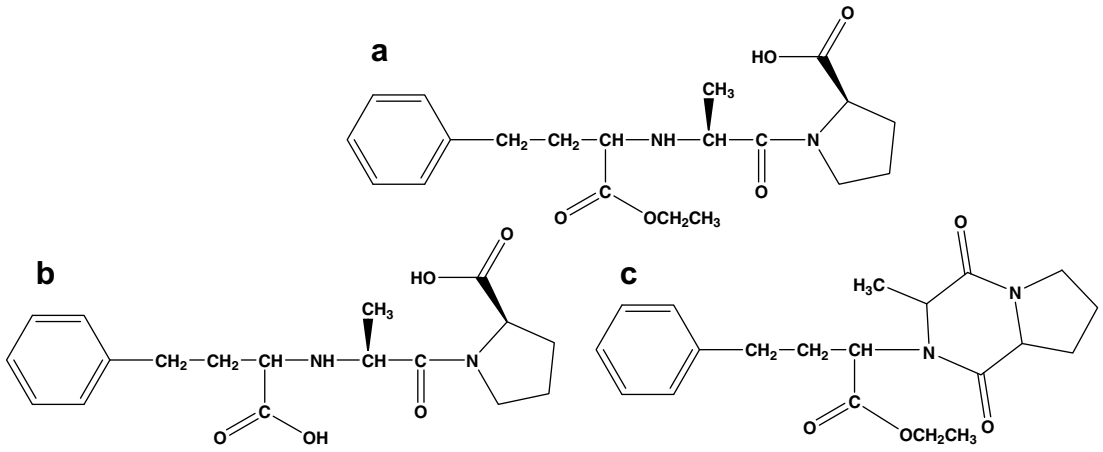

Figure 1. Molecular structure. (a) Enalapril, (b) enalaprilat and (c) diketopeparazine.

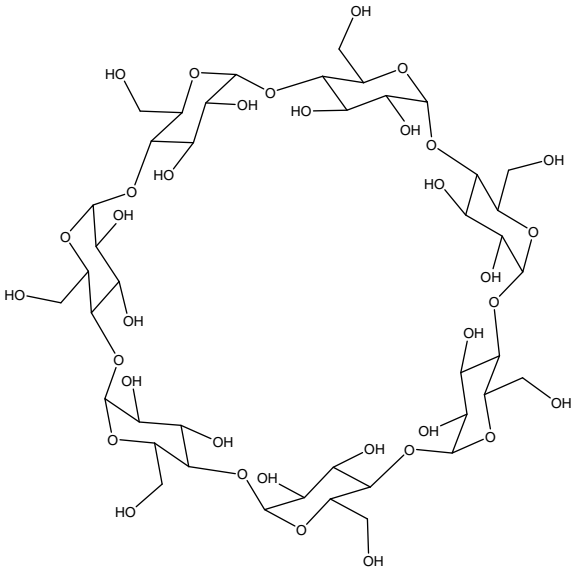

Figure 2. Molecular structure of β-CD.

tive insight into their structure, as well as their thermodynamic and kinetic properties.[13]

2.1.1.1. ^{1}H NMR studies. In order to study the structure of the ENA:β-CD complex, the spectra of pure ENA and β-CD were compared to their corresponding signals in the inclusion complex. c*is–trans* Isomerization may occur in proline-containing molecules such as ENA, with this drug being present in an aqueous solution as a mixture of the *Z-(cis)* and *E-(trans)* isomers (Fig. 3). Therefore, when possible, the signals corresponding to each isomer were identified.

As can be seen in Table 1, in the presence of β-CD, almost all ENA proton resonances were modified, and exhibited both upfield and downfield displacements with respect to those of the pure drug. Among the protons that had the most marked upfield displacement were those corresponding to the aromatic ring (H17′19′ and H16′18′20′), indicating that this moiety was located in a rich electronic density environment that produced a shielding effect. This evidence suggests that the aromatic ring of ENA may have been included into the β-CD hydrophobic cavity, near the glycosidic linkage oxygens that are rich in π electrons. A lower upfield displacement was observed for H14′, which indicates that the alkyl chain that connects the benzyl ring with the rest of the molecule was still buried into the β-CD cavity, but was closer to the wide rim of the molecule torus. On the other hand, a downfield displacement was observed for H9′, H11′ and H12′ protons demonstrating a deshielding effect, which might be explained by the presence of hydrogen bond interactions between the carbonyl group of the ethyl ester moiety in ENA and the hydroxyl groups of β-CD. Based on the additional downfield displacement observed for H2′, H7′ and H8′, we can postulate that the secondary amine and carbonyl moieties of the amide and carboxylic group also established hydrogen bond interactions with the hydrophilic rim of the macromolecule. The displacement of the chemical shifts for H3′, H4′ and H13′ was difficult to calculate due to these signals being multiplets, while those for H7′ and H5′ protons could not be determined because of peak overlapping with β-CD protons.

The analysis of the signals corresponding to β-CD also sheds lights on the structure of this complex. β-CDs are toroidal molecules (Fig. 4) with a truncated cone shape, with CH groups carrying

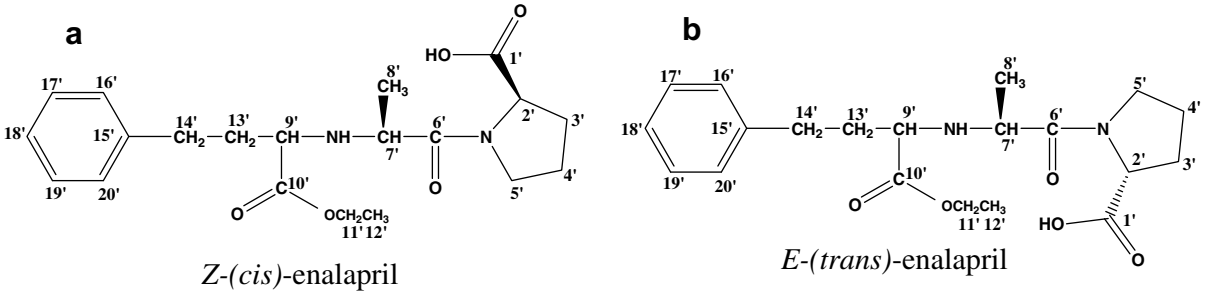

Figure 3. NMR signal notation. ENA isomers (a) *Z-(cis)* and (b) *E-(trans)*.

Table 1
Chemical shifts for the protons of ENA in the free state and in the 1:1 complex

Protons of ENA	ENA free (ppm)	ENA complex (ppm)	$\Delta\delta$ (ppm)
$H8'_E$	1.2546	1.2691	0.0145
$H8'_Z$	1.2716	1.2926	0.021
H12′	1.2935	1.3167	0.0232
H14′	2.7498	2.7388	−0.011
$H9'_Z$	3.2051	3.2722	0.0671
$H9'_E$	3.3939	3.4303	0.0364
H11′	4.1760	4.2014	0.0254
H2′	4.2566	4.2905	0.0339
H17′19′	7.3234	7.2864	−0.037
H16′18′20′	7.4021	7.3764	−0.0257

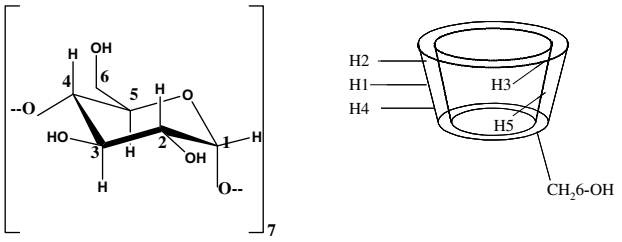

Figure 4. Molecular structure, NMR signal notation and schematic representation of the β-CD.

Table 2
Chemical shifts for the protons of β-cyclodextrin in the free state and in the 1:1 complex

Protons of β-CD	β-CD free (ppm)	β-CD complex (ppm)	$\Delta\delta$ (ppm)
H1	5.1000	5.0902	−0.0098
H2	3.6793	3.6696	−0.0097
H3	3.9951	3.9480	−0.0471
H4	3.6133	3.6086	−0.0047
H5	3.8837	3.7641	−0.1196
H6	3.9078	3.8698	−0.0380

the H1, H2 and H4 protons located on the exterior surface of the torus, which is of a hydrophilic nature. The interior of the torus is lined with two rings of CH groups (bearing H3 and H5) and also with glycosidic oxygens (O4), thus offering an environment of much lower polarity than that of water, and therefore can be considered to be of hydrophobic nature. Table 2 shows the displacements of the chemical shifts for β-CD protons in the presence or absence of ENA. A marked upfield displacement for H3, H5 and H6 is observed, which could be due to the inclusion into the β-CD hydrophobic cavity of groups that are rich in π electrons, such as the aromatic ring of ENA. As was expected, only small changes in the chemical shifts were observed for the H1, H2 and H4 protons located outside the cavity.

In order to assess the stoichiometry of the complex, Job's method was applied.[14] The continuous variation plots for the protons of ENA and β-CD, whose chemical shift displacements were the most marked, are shown in Figure 5. It can be observed that the maximums for both plots were found at $r = 0.5$, indicating a 1:1 stoichiometry for the ENA:β-CD complex.

Figure 6 shows Scott's plots for the ENA:β-CD complex, which were obtained based on the H-$9_{E/Z}$ and H-$8_{E/Z}$ protons of ENA. K_c values were then estimated from these plots and are presented in Table 3. The greater K_c value calculated for the complex with the *Z-(cis)* ENA isomer, compared to that of the *E-(trans)* isomer, may be due to the fact that the former is more hydrophobic than the latter one.[15]

2.1.1.2. ROESY. To study the spatial interaction between host and guest, and the corresponding three-dimensional geometry of the complex, a 2D ROESY experiment was carried out (Fig. 7). ROESY is a two-dimensional technique based on the Nuclear Overhauser Effect (NOEs), in which cross-peaks may be observed between protons if the corresponding internuclear distance is smaller than 3–4 Å.[16] An expansion of the ROESY spectrum obtained is shown in Figure 7b, where an interaction between the aromatic protons of ENA (H16′–H20′) and H3, H5 and H6 protons

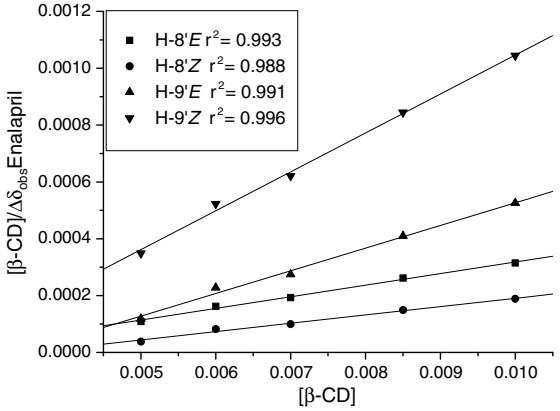

Figure 6. Scott's plots for the protons H-$9'_Z$ (●), H-$9'_E$ (■), H-$8'_Z$ (▼) and H-$8'_E$ (▲) of ENA with increasing concentrations of β-CD.

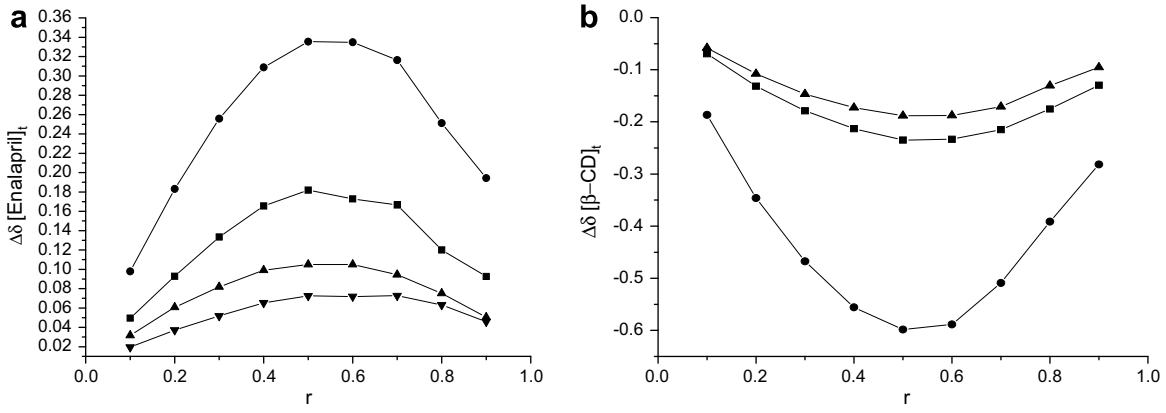

Figure 5. Continuous variation plot for (a) $H9'_E$ (■), $H9'_Z$ (●), $H8'_Z$ (▲) and $H8'_E$ (▼) protons of ENA in the presence of different relative concentrations of β-CD, (b) H3 (■), H5 (●) and H6 (▲) protons of β-CD in the presence of different relative concentrations of ENA.

Table 3
Complex formation constant for the inclusion complex of *Z*-(*cis*) and *E*-(*trans*) ENA with β-CD

Proton of ENA	Complex formation constant (M^{-1})
H-9_E	285
H-9_Z	455
H-$8'_E$	295
H-$8'_Z$	423
E-trans	290 ± 7
Z-cis	439 ± 23

of β-CD was found, indicating that the aromatic ring of the drug is deeply internalized into the cyclodextrin cavity.

Figure 7c, shows the intermolecular cross-peaks corresponding to the alkyl chain connecting the aromatic ring of ENA, in which an interaction was found between H14′ with H3 and H5, suggesting that this methylene group is also deeply inserted into the β-CD cavity. On the other hand, H13′ only exhibited correlations with the H3 proton, indicating that it is located closer to the wide rim of the molecule torus, and is thus not so deeply inserted into the hydrophobic cavity.

2.1.2. Computational studies

In order to obtain the initial conformation of ENA, a conformational search was performed over all the rotatable bonds in the molecule. In this way, we found that the Z-(*cis*) conformation was energetically favored at pH 7.0 respect to the *E*-(*trans*) conformation, and thus the former was used to initiate the docking studies.

On analyzing the carbon and oxygen affinity grids to be used in the docking procedures (Fig. 8a and b), we were able to confirm that carbon atoms are preferably accommodated in the interior cavity of the β-CD torus (hydrophobic cavity), while oxygen atoms are preferably located near the hydroxyl functional groups in the outer rim of the molecule.

2.1.2.1. Docking studies. From the results obtained by the docking procedures, we found three clusters of conformations for the ENA:β-CD complex (Fig. 9a–c). As can be seen, clusters of conformations were found corresponding to complexes in which the aromatic ring (a), the proline (b) and the ethyl ester moiety (c) are included into the β-CD hydrophobic cavity. By analyzing the docked energy values, it was concluded that the

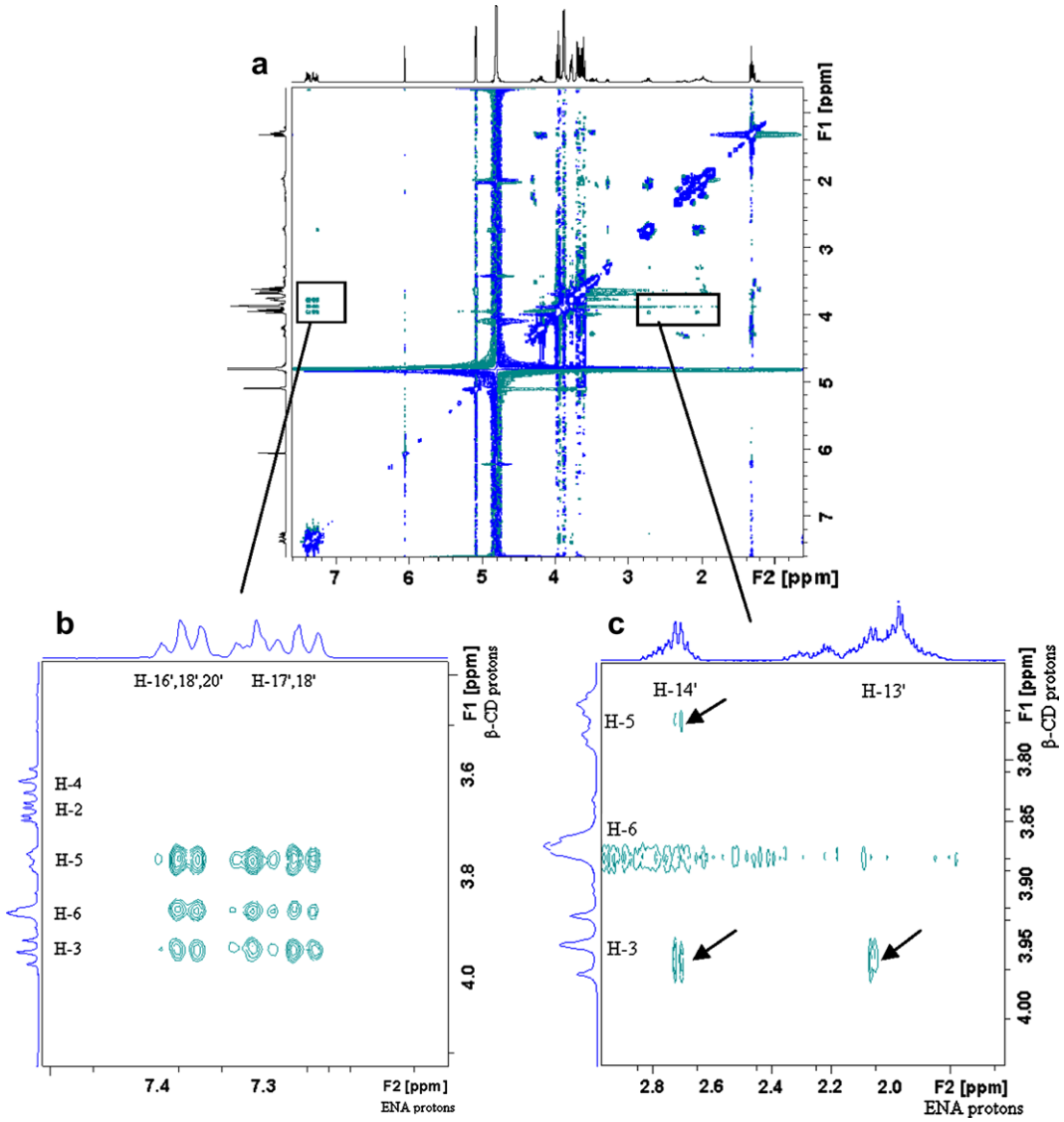

Figure 7. (a) 2D ROESY spectrum of ENA:β-CD complex. Expansion from the 2D ROESY spectrum of ENA:β-CD complex. (b) In F1 are shown protons H3, H5 and H6 of β-CD, and in F2 protons H16′,18′,20′ and H17′,19′ of ENA (c) in F1 are shown protons H3, H5 and H6 of β-CD, and in F2 protons H13′ and H14′ of ENA.

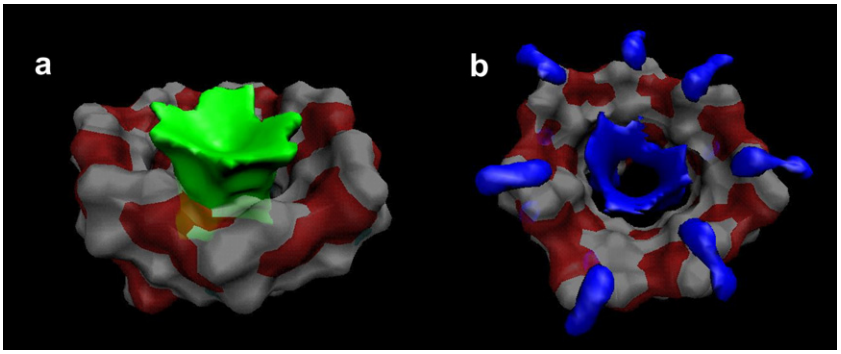

Figure 8. (a) Carbon affinity map located inside the β-CD cavity (hydrophobic) and (b) oxygen affinity map located near the outer rim of the torus (hydrophilic).

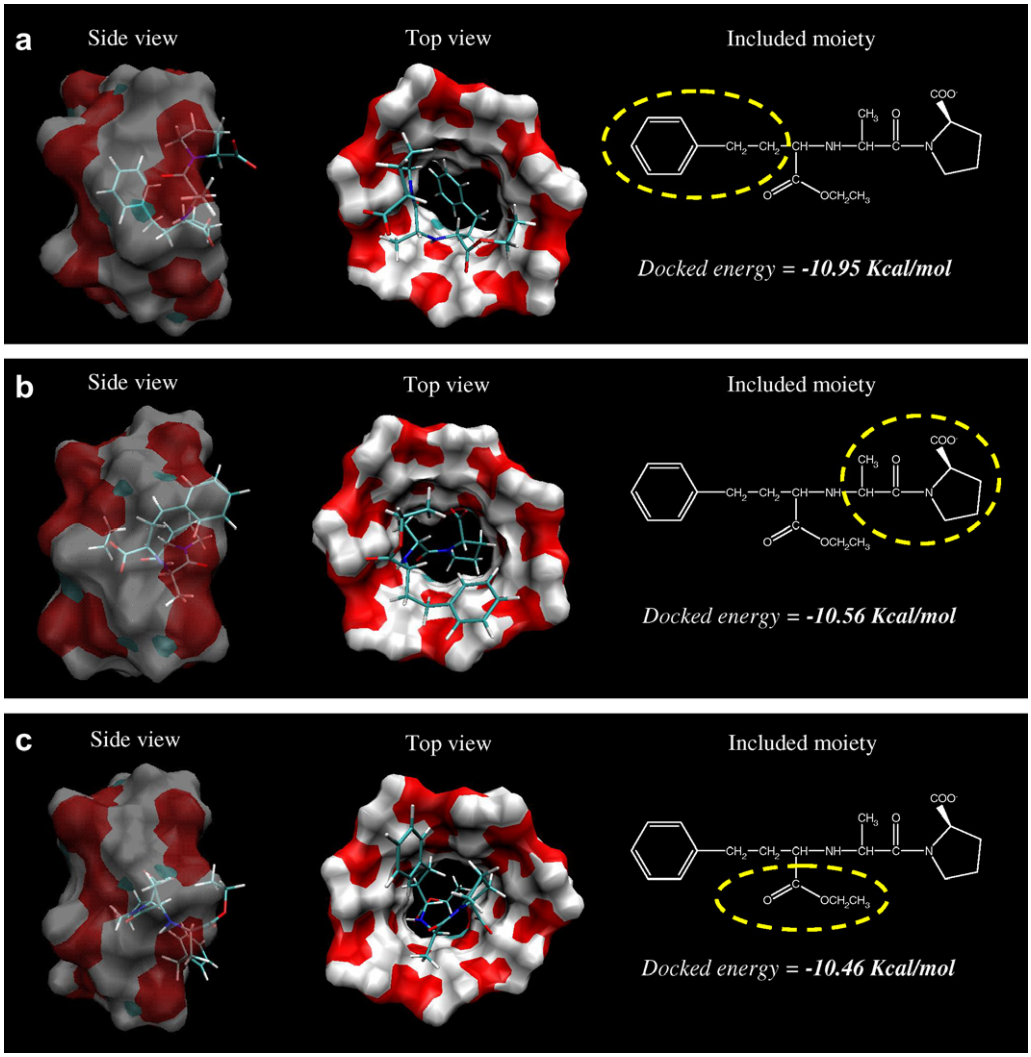

Figure 9. Three-dimensional conformation of the complexes between the *Z-cis* isomer of ENA and β-CD (clusters a, b and c) obtained by molecular docking.

complex in which the aromatic ring of ENA was included into the hydrophobic cavity of β-CD (a) was slightly more stable than the other two conformations. Considering the standard error associated to the quantitation of the docked energy reported for autodock3 (around 2.00 kcal/mol), one would expect that these conformations are equally probable. Therefore, in order to gain insight into the most stable complex, these three conformations obtained by molecular docking were refined, to include the effect of the presence of explicit solvent molecules, temperature and β-CD flexibility. Thus, the three clusters obtained were subjected to posterior refinement by means of molecular dynamics methods.

2.1.2.2. Molecular dynamics studies. The quality of the molecular dynamics trajectories corresponding to the clusters (a), (b) and (c) were evaluated by analyzing the temperature, and kinetic,

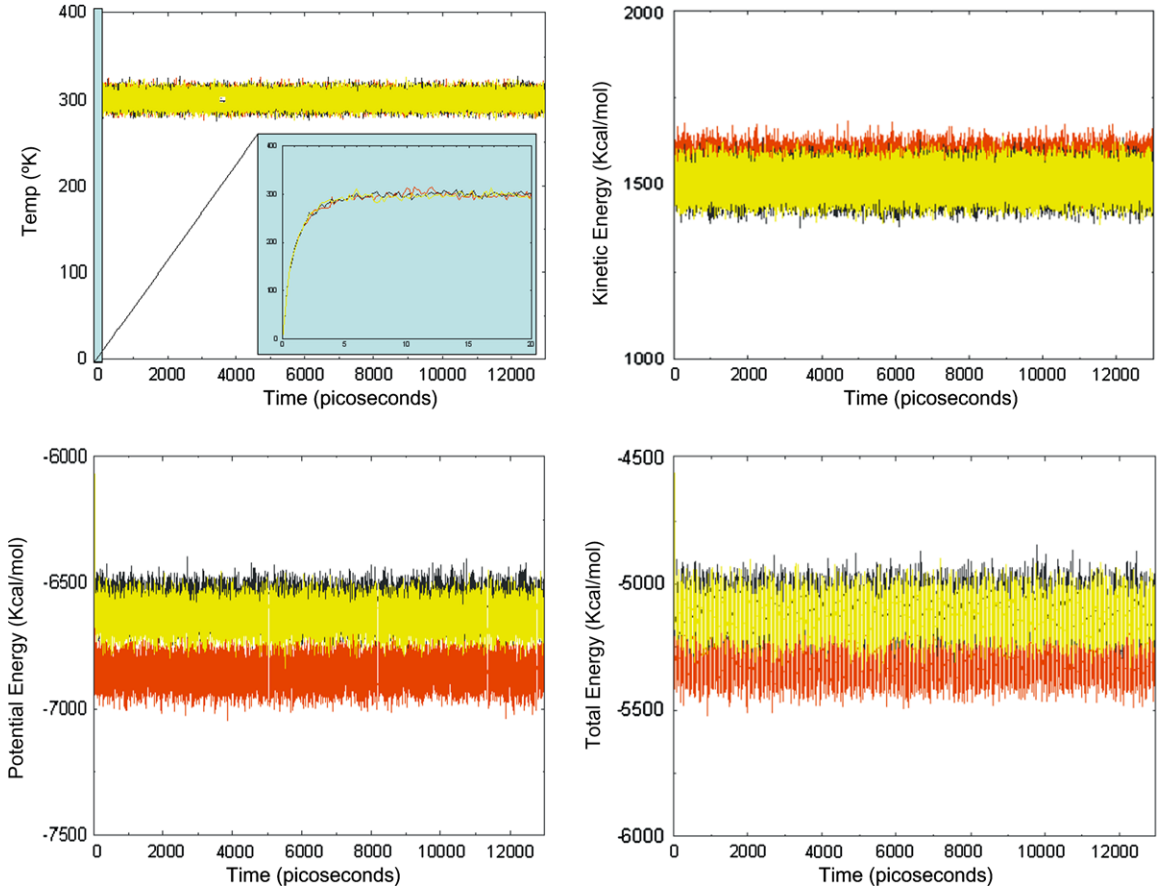

Figure 10. Plots of temperature, kinetic energy, potential energy and total energy for the molecular dynamics simulations of the ENA:β-CD complex (Cluster (a) (red), (b) (black) and (c) (yellow)).

potential and total energy profiles for 13 ns of simulation (Fig. 10a–d). As can be seen, no abnormal events occurred during the heating, equilibration on production runs, indicating that the conditions under which the trajectories were obtained were adequate. For the next step, the rmsd versus time profiles (Fig. 11a–c) were constructed and analyzed in order to evaluate if any significant conformational change occurred in the complex during the molecular dynamics run. From the plots in Figure 11, it can be seen that cluster (a) shows a slight change in its structure at around 5 ns, with the benzyl ring now being accommodated deeply into the β-CD hydrophobic cavity, with this conformation becoming stable after 6 ns. When cluster (b) was analyzed, we found that a considerable conformational fluctuation occurred up to 7 ns of simulation, in which the proline moiety moved toward the wide rim of the torus, thereby optimizing the establishment of new hydrogen bond interactions. Cluster (c) exhibited a considerable increase in its rmsd between 3 and 4 ns, which was due to the exclusion of the ethyl ester moiety of ENA from the β-CD hydrophobic cavity.

2.1.2.3. Energetic component analysis. Following on from the aspects discussed with respect to the rmsd versus time plots, energetic component analyses (MM-PBSA) were performed over the time interval corresponding to 7–13 ns of simulation (Table 4). When the total free energy of binding for the three clusters was compared, we found that cluster (a) was clearly favored, with an energy of −18.63 kcal/mol. This was followed by cluster (b) with an energy of −16.00 kcal/mol. The factibility of the formation of the cluster (c) is discarded based on two observations. First, it was been demonstrated that ENA was excluded from the β-CD cavity during the simulation, and secondly, it was found to be less favorable on analysis of the total binding energy (−10.98 kcal/mol).

Based on the energetic component analysis, we conclude that the complex conformation in which the aromatic ring of ENA is included into the β-CD hydrophobic cavity is the favored conformation. Although the electrostatic component for cluster (a) was considerably lower than that of cluster (b) (−28.92 and −95.34 kcal/mol, respectively), the Van der Waals component was higher (−25.38 and −15.13 kcal/mol, respectively). A main force that drove the complex formation was the solvation component, which was positive for the three evaluated conformations. However, considering that the most hydrophobic part of the ENA molecule was the aromatic ring, do to its inclusion into the hydrophobic cavity and removal from the bulk of the water molecules, then as expected, the energy required to solvate the ligand during the complex formation was discovered to be considerably lower in cluster (a) compared to (b) (36.33 kcal/mol and 95.04 kcal/mol, respectively). Related to this, the solvation energy dependence for the formation of cyclodextrin inclusion complexes has been previously described.[13] The formation of complex (a) is in agreement with spectroscopic data, which indicated that the aromatic ring is included into the β-CD hydrophobic cavity. This was confirmed by observing the upfield displacement in H16′–H20′ protons of the ENA molecule, as well as using data provided by the 2D ROESY experiments.

2.1.2.4. Effect of the *cis*/*trans* isomerism in the complex formation. As can be seen in Table 3, the formation constant for the complex corresponding to the *Z-cis* conformation of ENA

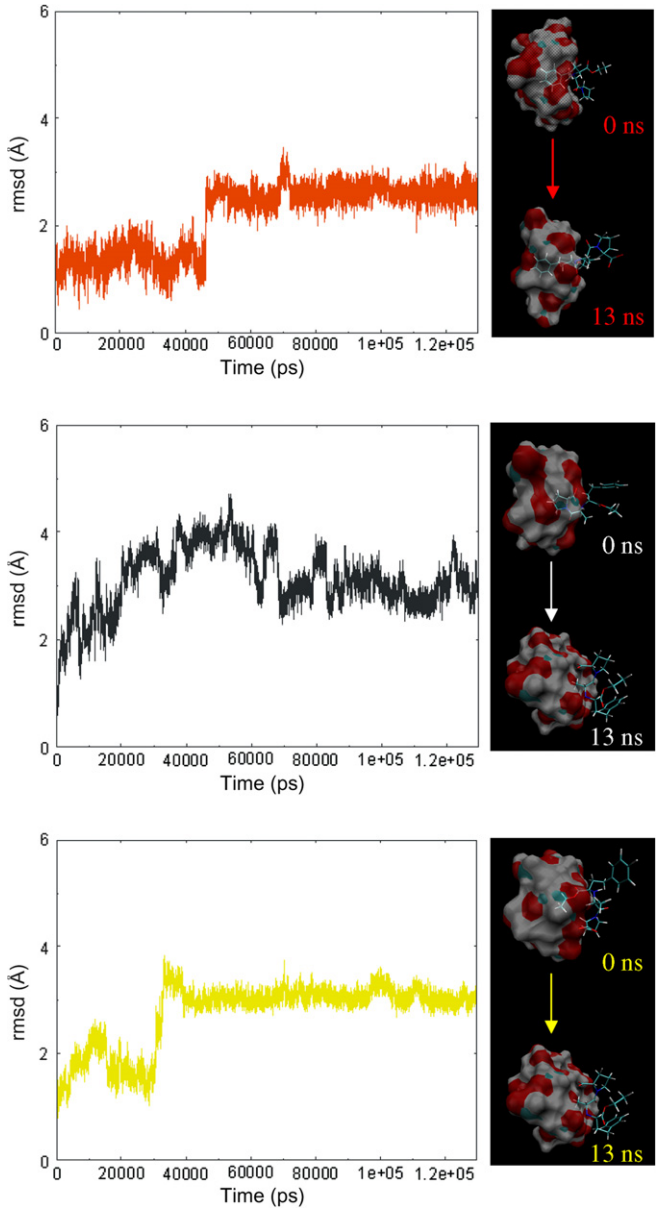

Figure 11. Plots of the root-mean-square deviation (RMSD) versus time for the three clusters of the ENA:β-CD complex subjected to molecular dynamics simulations.

Table 4
Energetic component analysis obtained by MM-PBSA for the three clusters of the ENA:β-CD complex analyzed by molecular dynamics simulations

Energetic component	Cluster (a) (kcal/mol)	Cluster (b) (kcal/mol)	Cluster (c) (kcal/mol)
Electrostatic	−28.92	−95.34	−101.36
Van der Waals	−25.38	−15.13	−6.99
Gas state total	−54.96	−111.04	−109.04
Polar and non-polar contrib.	36.33	95.04	98.06
Free energy of binding	−18.63	−16.00	−10.98

is higher than that of the *E-trans* isomer. In order to study the structural basis of this observation, the *E-trans* isomer was docked to the β-CD molecule, and then the same molecular dynamic and energetic component analysis was performed as described above. The docking pose thus obtained was similar to that of the *Z-cis* isomer, with the benzyl ring of the ENA molecule being inserted deeply into the β-CD cavity, and the proline moiety being positioned near the hydrophilic ring of the torus. After 13 ns of molecular dynamics simulations and also using the MM-PBSA analysis, we found a free energy of binding of −15.81 kcal/mol, which compared to the value obtained for the *Z-cis* conformation (−18.63 kcal/mol), thereby supporting the higher formation constant found for the latter. When analyzing the corresponding energetic components, we found electrostatic, Van der Waals and polar/non-polar contribution of −37.02, −27.49 and 48.70 kcal/mol, respectively. Based on these data, we can conclude that the force driving the ENA:β-CD complex formation (polar and non-polar solvation energy) was also due to the higher affinity of the *Z-cis* conformation of ENA when complexed to β-CD, since the energy necessary to solvate the *E-trans* isomer was higher than that of its counterpart, the *Z-cis* one (48.70 and 36.33 kcal/mol, respectively).

2.2. Complex formation in solid state

2.2.1. IR studies

The reported lyophilization method resulted in a simple and convenient way to obtain the complex between ENA and β-CD in the solid state. The formation of this complex may be studied by IR spectroscopy based on the ligand, since it possesses carbonyl functional groups that present bands between 1680 and 1700 cm^{-1}, which can be significantly modified as a consequence of complexation.[13]

Due to the fact that ENA showed three important bands at 1753, 1728 and 1647 cm^{-1} (Fig. 12 a), which were attributed to carbonyl stretching of the carboxylic acid, ester and tertiary amide, respectively, then the modification of these signals may be used to identify the establishment of intermolecular interactions involving these groups, thus confirming the formation of an inclusion complex. The infrared spectra of different samples are presented in Figure 12. As shown in the spectra for the physical mixture, it consists of an overlay of the pure compound spectra whereas the spectrum of the complex shows differences from that of pure ENA. For the IR spectrum corresponding to the ENA:β-CD complex, it is observed that the band at 1753 cm^{-1} is not present, but two new bands, due to the formation of the carboxylate anion, become visible at 1550 and 1400 cm^{-1}. Also, the bands at 1728 and 1647 cm^{-1} became broader and were shifted to lower frequencies. This spectral shift may have originated from the establishment of stable hydrogen bond interactions be-

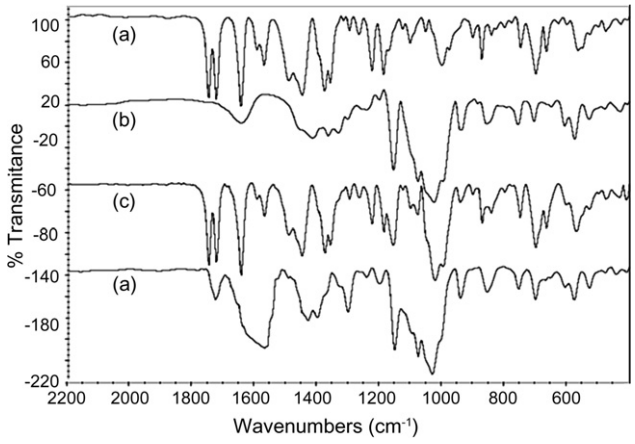

Figure 12. IR spectra of (a) ENA, (b) β-CD, (c) ENA:β-CD physical mixture and (d) ENA:β-CD freeze-dried complex.

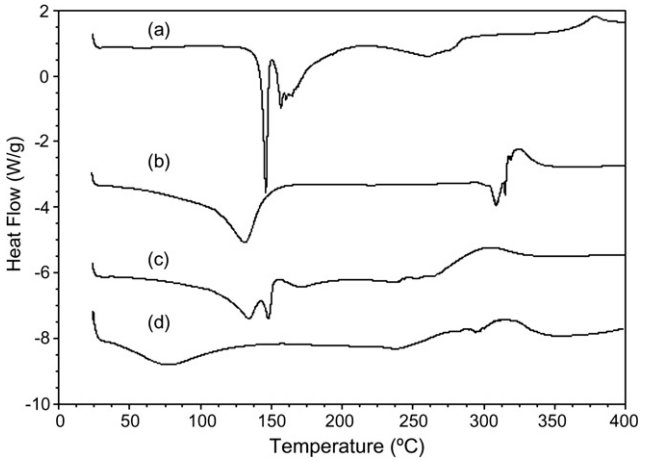

Figure 13. DSC curves of (a) ENA, (b) β-CD, (c) ENA:β-CD physical mixture, (d) ENA:β-CD freeze-dried complex.

tween ENA and β-CD. Furthermore, a reduction of the intensities of the vibrational bands of ENA was observed for the complex, a fact that is consistent with the vibrational constrictions imposed on the guest molecule in the cyclodextrin cavity. Based on this evidence, we can confirm the existence of intermolecular interactions between ENA and β-CD, and consequently the formation of the corresponding inclusion complex.

2.2.2. DSC and TGA studies

The DSC and TGA curves of pure ENA, pure β-CD, their physical mixture, and the corresponding inclusion complex are shown in Figures 13 and 14, respectively. The DSC curve of pure ENA shows a sharp endothermic peak at 146 °C, corresponding to its melting, thus demonstrating its crystalline anhydrous state. From 153 °C, another endothermic shoulder is observed, with a maximum at 163 °C, while the TGA curve showed a loss of the mass fraction of 29% during this temperature interval. As was previously proposed by Lin et al.,[17] the observed features for free enalapril maleate may be indicating a complex reaction that includes the formation of diketopiperazine.

When analyzing the DSC and TG curves of β-CD, it can be seen that between 50 and 150 °C an endothermic event takes place, with a weight loss of 11% of the mass fraction, corresponding to its water content. Decomposition of β-CD occurs over 300 °C. Also expected when analyzing the physical mixture of ENA and β-CD, the characteristic events observed for the pure compounds were found.

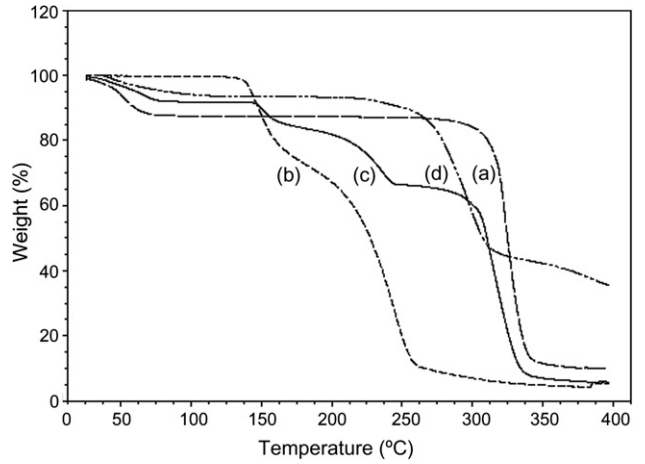

Figure 14. TG curves of (a) β-CD (— —), (b) ENA (----), (c) ENA:β-CD physical mixture (——) and (d) ENA:β-CD freeze-dried complex (— – —).

For the results obtained for the complex prepared by lyophilization, the DSC curve shows that the endothermic peak of pure ENA at 146 °C is not present, indicating that the melting event did not take place, which might be due to changes in the crystalline form of the solid, or to an inclusion complexation. Also, the TGA curve shows that the decomposition of ENA starts at above 235 °C, a temperature that is considerably higher than that for pure ENA (153 °C). This fact indicates that the formation of the inclusion complex considerably enhances the stability of ENA in solid state. In addition, these observed curve patterns are in agreement with IR spectroscopic data with respect to the formation of the inclusion complex.

2.3. Stability studies

After performing the corresponding stability assay, we found that the main degradation product of ENA in pH 7.0 buffer solution was ET, with a retention time of 0.8 min. This observation was consistent with bibliographic data.[1]

The corresponding degradation rates for free ENA (k_o) and for the ENA:β-CD complex at different β-CD concentrations (k_{obs}) were calculated (Fig. 15). In both cases, a pseudo first-order kinetic degradation behavior was found, demonstrating that the presence of β-CD did not influence the reaction order or the degradation mechanism.

Considering that we previously determined that the complex has a 1:1 stoichiometry, we then applied the values obtained for k_o and k_{obs} in order to calculate the corresponding formation constant of the complex (K_c) and the degradation rate of the drug within it (k_c), at 70 °C as described by Loftsson and Brewster[10] In this way, free ENA exhibited a shelf life time (t_{90}) of 6.7 h ($k_o = 1.56 \times 10^{-2}\ h^{-1}$), while the drug within the complex showed a t_{90} of 14 h ($k_c = 0.74 \times 10^{-2}\ h^{-1}$). This allows us to conclude that the drug complexed with β-CD is 2.1 times more stable than its free counterpart.

3. Conclusion

From the results present, we can conclude that the production of an inclusion complex between enalapril maleate and β-CD was achieved by applying a lyophilization method, which might be of use at an industrial scale.

Taking into account the stability issues of ENA, we found that the strategy applied in this work resulted in an enhanced stability of the drug, not only in solid state as observed in the thermal analysis studies, but also in solution as described in the accelerated degradation experiments. These observations suggest that the formulation of ENA with β-CD may overcome the problems currently described for solid dosage forms of this drug, and also provides an interesting alternative for the preparation of orally administered solutions of ENA.

Additionally, we were able to successfully combine molecular modeling studies with experimental spectroscopic assays, in order to elucidate the molecular bases and thereby explains the complex formation and the specific intermolecular interactions taking place. The methodology applied might then be extensible to the preparation of β-CD inclusion complexes with other molecules that exhibit similar stability issues, thus allowing a preliminary computational study of the potential complex.

Finally, we can postulate that the preparation of an oral dosage containing the ENA:β-CD complex could be very useful for the treatment of essential and renovascular hypertension, although further physical and chemical studies are needed to assess the bioavailability of ENA from the complex.

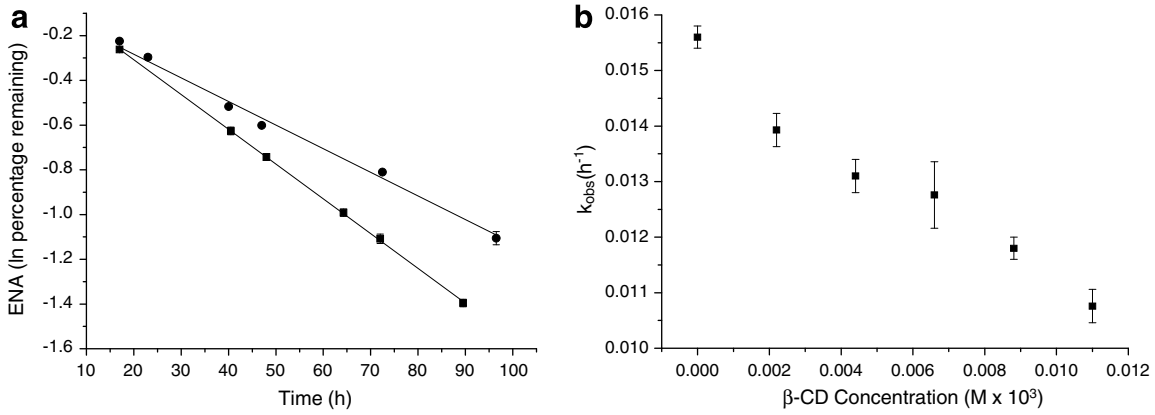

Figure 15. (a) Plot of pseudo first-order kinetic degradation of ENA, (■) free and in the presence of β-CD 11 mM (●) and (b) plot of k_{obs} versus β-CD concentration for the degradation of ENA.

4. Materials and methods

4.1. Materials

Enalapril maleate, D_2O 99.9 atom% D, and NaOD 40% used in spectroscopic studies were purchased from Sigma®, while β-CD (M_W = 1135) was kindly supplied by Roquette (France). All other materials and solvents were of analytical reagent grade. A Milli-Q Water Purification System (Millipore®, USA) generated the water used in these studies. Also a H_2KPO_4/HK_2PO_4 pH 7.0 buffer was used (pH-meter ORION SA520, USA), with its ionic strength being adjusted to 0.5 by addition of KCl.

4.2. NMR studies

All experiments were performed on a Bruker® Avance II High Resolution Spectrometer, equipped with a Broad Band Inverse probe (BBI) and a Variable Temperature Unit (VTU). The spectra were measured at 298 K, adjusting the solutions to pD 7.0 by the addition of $NaOD/D_2O$.

4.2.1. ^{1}H NMR

Spectra were obtained at 400.16 MHz, with the chemical shift of the residual solvent at 4.8 ppm used as an internal reference. Induced changes in the ^{1}H chemical shifts for ENA and β-CD ($\Delta\delta$) originated due to their complexation were calculated using the following equation:

$$\Delta\delta = \delta_{complex} - \delta_{free} \quad (1)$$

The stoichiometry of the complex was studied by applying the continuous variation method,[14] using the NMR spectra obtained for a series of ENA and β-CD mixtures in which the sum of their concentrations was kept constant at 10 mM, but varying their molecular fraction between 0 and 1. After registering the corresponding changes in the most sensitive NMR signals, the stoichiometry of the inclusion complex was calculated.

The apparent formation constant (K_c) of the inclusion complex in solution was determined by applying Scott's equation (Eq. (2))[18]:

$$\frac{[\beta\text{-CD}]_t}{\Delta\delta_{obs}} = \frac{[\beta\text{-CD}]_t}{\Delta\delta_c} + \frac{1}{K_c\Delta\delta_c} \quad (2)$$

where $[\beta\text{-CD}]_t$ is the total β-CD concentration; $\Delta\delta_{obs}$ is the difference between the chemical shift of free ENA and the corresponding chemical shift of ENA in the presence of β-CD at each concentration; $\Delta\delta_c$ is the difference between the chemical shift of a pure sample of the complex and its free components. By plotting $[\beta\text{-CD}]_t/\Delta\delta_{obs}$ against $[\beta\text{-CD}]_t$, K_c could be calculated from the intercept obtained by a least squares linear analysis. In this experiment, the concentration of ENA was kept constant at 2 mM, while β-CD concentration was varied from 5 to 10 mM for the D_2O of pD 7.0.

2D ROESY: the geometry of the inclusion complex was studied by two-dimensional Rotating frame Overhauser experiments (2D ROESY), with spinlock for mixing phase sensitive, using $180x\ 180 - x$ pulses for polarization transfer. The spectra were measured with a relaxation delay of 2 s, p15 pulse for ROESY spinlock of 20 ms and l4, spinlock loop, (p15/p25 * 2) = 400.

Before Fourier transformation, the matrix was zero filled to 4096 (F2) by 2048 (F1) and Gaussian apodization functions were applied in both dimensions. Working concentrations of both ENA and β-CD were 5 mM in D2O, at pD 7.0.

4.3. Molecular modeling procedures

The initial molecular structure of ENA was built using the graphical interface Gabedit, after which a systematic conformational search was performed in order to obtain the minimum energy conformation. In this way, a semiempirical method (AM1) was applied during the conformational search, with the final minimum energy conformation being optimized using an ab-initio (HF-6-31G*) method. Both semiempirical and ab-initio methods are implemented in the Gaussian 98 software.[19] The initial structure of β-CD was obtained from the Cambridge Structural Database (PDB code BCDEXD10).

For the molecular docking procedure, restrained electrostatic potential (RESP) fitted charges were assigned to ENA, while for β-CD, charges corresponding to the Glycamm04 force field implemented in the Amber9 software package were assigned.[20] Autodock v3.05 was used to perform the dockings runs,[21] by applying a Lamarckian Genetic Algorithm (LGA) to generate the population evaluated, using the following parameters: a population of 150 individuals, a maximum numbers of 250,000,000 evaluations and 5000 generations as an end criterion. An elitism value of 1 was selected, with a probability of mutation and crossing over of 0.02 and 0.8, respectively. Thirty docking runs were performed, and the three lowest energy cluster conformations were selected for posterior molecular dynamics assays.

The Amber9 software package was used for the molecular dynamics studies.[20] Atomic charges for ENA and β-CD were identical to those used for the molecular docking procedures described above. The complexes obtained by molecular docking were solvated with a pre-equilibrated TIP3P octahedric water box, by performing an initial minimization of the solvent followed by a minimization of the whole system. These minimized systems were

heated to 300 K for 20 picoseconds (ps), followed by a 100 ps equilibration run. Production runs were performed for 13 nanoseconds (ns), using a timestep of 2 femtoseconds (fs) and under constant pressure and temperature, with the SHAKE algorithm being applied to constrain bonds involving hydrogens. The trajectories obtained were monitored by plotting temperature, total energy, potential energy and root-mean-square deviation (rmsd) of the corresponding structures.

The hydrogen bond and energetic component analyses were performed using the Ptraj and Molecular Mechanics Poisson-Boltzmann Surface Area (MM-PBSA) modules of Amber9, respectively.[20] MM-PBSA analyses were performed over a 4 ns segment, with individual snapshots sampled every 10 frames of the trajectory. The corresponding structures were visualized using the VMD software.[22] Molecular dynamics simulations were performed at the Fimm Cluster resource (Parallab, Bergen Center for Computational Science, University of Bergen, Norway).

4.4. Preparation of the ENA:β-CD complex in solid state

A solution of ENA and β-CD (1:1 molar ratio) was prepared in distilled water, and the pH 7.0 was adjusted by addition of NaOH 1 N. The resulting solution was placed in an ultrasonic bath for 1 h, after which it was incubated at 25.0 (±0.1) °C in a thermostatic water bath (Circulators HAAKE F3-K, Germany) for 48 h. Then, the solutions were frozen at −40 °C before being freeze-drying started (Freeze Dri 4.5 Labconco Corp., Kansas City, MI).

4.5. Fourier transform infrared spectroscopy (FT-IR)

The FT-IR spectra of ENA and its complex with β-CD were measured as potassium bromide disks on a Nicolet 5 SXC FT-IR Spectrometer. The FT-IR spectrum of ENA:β-CD was compared with those of the corresponding 1:1 molar ratio physical mixture and also with pure ENA and β-CD. All spectra were obtained and processed using EZ OMNIC E.S.P v.5.1 software.

4.6. Differential scanning calorimetry (DSC) and thermogravimetric analysis (TGA)

The DSC curves of the different samples were recorded on a DSC TA 2920 and the TGA curves on a TG TA 2920, both by applying a heating rate of 10 °C min^{-1}. The thermal behavior was studied over a temperature range of 25–400 °C, by heating 1–3 mg of samples in aluminum-crimped pans under nitrogen gas flow. Data were obtained and processed using the TA Instruments Universal Analysis 2000 software.

4.7. Stability studies

The chemical stability of ENA complexed to β-CD was determined at 70 °C in pH 7.0 phosphate buffer solutions containing β-CD concentrations of between 0 and 11 mM. Solutions were prepared by dissolving 20 mg of enalapril maleate in 100 ml of the aqueous buffer containing the desired β-CD concentration, which were then placed in a thermostated water bath (Circulators HAAKE F3-K, Germany). Samples were taken at various time intervals.

The quantitation of ENA was carried out by applying the HPLC method reported by Pilatti et al.,[9] with minor modifications. The HPLC equipment consisted of an Agilent S1100 system with UV detection at 215 nm, using a Zorbax Eclipse XDB-C8 (4.6 × 150 mm, 5 μm, Agilent Technologies, USA) reversed-phase column. The mobile phase was an acetonitrile:pH 2.2 potassium phosphate buffer (10 mM) 32:68 mixture, at a flow rate of 2.0 ml/min. Assays were performed at 60 °C, by injecting 50 μl of solution in each chromatographic run. Under these conditions, the retention times for ET, ENA and DKP were 0.8 min, 1.5 min and 5.0 min, respectively.

The observed first-order rate constant for degradation of free ENA (k_0) and ENA complexed with β-CD (k_{obs}) were determined by applying a linear regression analysis for the plots of the natural logarithm of the remaining ENA concentration versus time. The complex formation constant (K_c) and the degradation of the drug within the complex (k_c) were calculated from Lineweaver–Burk plots.[10]

Acknowledgments

The authors thank the Secretaría de Ciencia y Técnica de la Universidad Nacional de Córdoba (SECyT), and the Consejo Nacional de Investigaciones Científicas y Tecnológicas de la Nación (CONICET) for financial support. We also thank the Ferromet S.A. (agent of Roquette in Argentina) for their donation of β-cyclodextrin. We would also like to specially thank Dr. Petter Bjorstad (Research Director at Bergen Center for Computational Science (BCCS)) for kindly providing the access to BCCS computing resources, and Dr. Paul Hobson, native speaker, for revision of the manuscript.

References and notes

1. *Analytical Profiles of Drug Substances*; Ip, D. P., Brenner, G. S., Florey, K., Eds.; Academic Press: New York, 1987; Vol. 16.
2. Al-Omari, M. M.; Abdelah, M. K.; Badwan, A. A.; Jaber, A. M. Y. *J. Pharm. Biomed. Anal.* **2001**, *25*, 893.
3. Wang, S. L.; Lin, S. Y.; Chen, T. F.; Cheng, W. T. *Pharm. Res.* **2004**, *21*, 2127.
4. Cotton, M. L.; Wu, D. W.; Vadas, E. B. *Int. J. Pharm.* **1987**, *40*, 129.
5. Stanisz, B. J. *Pharm. Biomed. Anal.* **2003**, *31*, 375.
6. Oliva, M. A.; Sombra, L. L.; Olsina, R. A.; Masi, A. N. *J. Fluoresc.* **2005**, *15*, 723.
7. Bhardwaj, S. P.; Singh, S. *J. Pharm. Biomed. Anal.* **2008**, *46*, 113.
8. Simoncic, Z.; Zupancic, P.; Roskar, R.; Gartner, A.; Kogej, K.; Kmetec, V. *Int. J. Pharm.* **2007**, *342*, 145.
9. Pilatti, C.; Ercolano, I.; Torre, M.; Del, C.; Chiale, C.; Spinetto, M. *Drug Dev. Ind. Pharm.* **1999**, *25*, 807.
10. Loftsson, T.; Brewster, M. E. *J. Pharm. Sci.* **1996**, *85*, 1017.
11. Vianna, R. F. L.; Bently, M. V. L. B.; Riebeiro, G. *Int. J. Pharm.* **1998**, *167*, 205.
12. Li, J.; Guo, Y.; Zografi, G. *J. Pharm. Sci.* **2002**, *91*, 229.
13. Fromming, K. H.; Szejtli, J. *Cyclodextrins in Pharmacy*; Kluwer Academic Publishers: Dordrecht, 1994.
14. Job, P. *Ann. Chim.* **1928**, *9*, 113.
15. Shoji, A.; Yanagida, A.; Shindo, H.; Ito, Y.; Shibusawa, Y. J. *Chromatogr. A* **2007**, *1157*, 101.
16. Scheider, H. J.; Hacket, F.; Rudiger, V.; Ikeda, H. *Chem. Rev.* **1998**, *98*, 1755.
17. Lin, S. Y.; Wang, S. L.; Chen, T. F.; Hu, T. C. *Eur. J. Pharm. Biopharm.* **2002**, *54*, 249.
18. Ganza-Gonzalez, A.; Vila-Jato, J. L.; Anguiano-Igea, S.; Otero-Espinar, F. J.; Blanco-Mendez, J. *Int. J. Pharm.* **1994**, *106*, 179.
19. Frisch, M. J.; Trucks, G. W.; Schlegel, H. B.; Scuseria, G. E.; Robb, M. A.; Cheeseman, J. R.; Zakrzewski, V. G.; Montgomery, J. A., Jr.; Stratmann, R. E.; Burant, J. C.; Dapprich, S.; Millam, J. M.; Daniels, A. D.; Kudin, K. N.; Strain, M. C.; Farkas, O.; Tomasi, J.; Barone, V.; Cossi, M.; Cammi, R.; Mennucci, B.; Pomelli, C.; Adamo, C.; Clifford, S.; Ochterski, J.; Petersson, G. A.; Ayala, P. Y.; Cui, Q.; Morokuma, K.; Malick, D. K.; Rabuck, A. D.; Raghavachari, K.; Foresman, J. B; Cioslowski, J.; Ortiz, J. V.; Baboul, A. G.; Stefanov, B. B.; Liu, G.; Liashenko, A. P.; Piskorz, I.; Komaromi, R.; Gomperts, R. L.; Fox Martin, D. J.; Keith, T.; Al-Laham, M. A.; Peng, C. Y.; Nanayakkara, A.; Gonzalez, C.; Challacombe, M.; Gill, P. M. W.; Johnson, B.; Chen, W.; Wong, M. W.; Andres, J. L.; Gonzalez, C.; Head-Gordon, M.; Replogle, E. S.; Pople, J. A. *Software: GAUSSIAN 98*; Gaussian, Inc.: Pittsburgh, PA, USA, 1998. www.gaussian.com.
20. Case, D. A.; Cheatham, T. E., III; Darden, T.; Gohlke, H.; Luo, R.; Merz, K. M.; Onufriev, A., Jr.; Simmerling, C.; Wang, B.; Woods, R. J. *Comput. Chem.* **2005**, *26*, 1668.
21. Morris, G. M.; Goodsell, D. S.; Halliday, R. S.; Huey, R.; Hart, W. E.; Belew, R. K.; Olson, A. J. *J. Comput. Chem.* **1998**, *19*, 1639.
22. Humphrey, W.; Dalke, A.; Schulten, K. *J. Mol. Graph.* **1996**, *14*, 33.